Chem Biol Drug Des 2011; **77:** 166–172

Research Article

doi: 10.1111/j.1747-0285.2010.01071.x

Synthesis of 2-Hydrazolyl-4-Thiazolidinones Based on Multicomponent Reactions and Biological Evaluation Against *Trypanosoma Cruzi*

Chiara Pizzo[1], Cecilia Saiz[1], Alan Talevi[2], Luciana Gavernet[2], Pablo Palestro[2], Carolina Bellera[2], Luis Bruno Blanch[2], Diego Benítez[3], Juan J. Cazzulo[4], Agustina Chidichimo[4], Peter Wipf[5] and S. Graciela Mahler[1,*]

[1]Departamento de Química Orgánica, Cátedra de Química Farmacéutica, Universidad de la República (UdelaR), Avda. General Flores 2124, CC1157 Montevideo, Uruguay
[2]Cátedra de Química Medicinal, Departamento de Ciencias Biológicas, Facultad de Ciencias Exactas, Universidad Nacional de La Plata (UNLP), La Plata, Argentina
[3]Laboratorio de Química Orgánica, Facultad de Ciencias-Facultad de Química, UdelaR, Montevideo, Uruguay
[4]IIB-INTECH Universidad Nacional de General San Martín – CONICET, San Martín, Argentina
[5]Department of Chemistry, University of Pittsburgh, Pittsburgh, PA 15260, USA
**Corresponding author: S. Graciela Mahler, gmahler@fq.edu.uy*

A series of 18 novel 2-hydrazolyl-4-thiazolidinones-5-carboxylic acids, amides and 5,6-α,β-unsaturated esters were synthesized, and their *in vitro* activity on cruzipain and *T. cruzi* epimastigotes was determined. Some agents show activity at 37 μM concentration in the enzyme assay. Computational tools and docking were used to correlate the biological response with the physicochemical parameters of the compounds and their cruzipain inhibitory effects.

Key words: 2-hydrazolyl-4-thiazolidinone, Chagas disease, cruzipain, inhibitors, multicomponent connection reaction, *Trypanosoma cruzi*

Received 19 August 2010, revised 8 December 2010 and accepted for publication 11 December 2010

A century after its discovery, Chagas disease still represents a major public health challenge in Latin America where currently an estimated 11 million people are currently infected. Because of growing population movements, an increasing number of Chagas disease cases have now been detected in non-endemic areas, such as North America and some European countries. Unfortunately, only benznidazole and nifurtimox are clinically available for treatment of the disease, and both demonstrate only limited efficacy during the acute phase of the disease and show severe side effects (1).

The growing knowledge of the basic biology of *Trypanosoma cruzi,* the ethiological agent causative of Chagas disease, empowers the development of new, rationally developed approaches to specific chemotherapy. The cathepsin L-like cysteine protease termed cruzipain or cruzain is responsible for the major proteolytic activity of all stages of the parasite life cycle and represents an interesting target for the development of potential therapeutics for the treatment of the disease (2). Cruzipain is differentially expressed in the four main stages of the parasite's biological cycle; it is located in different cellular compartments and is essential for the survival of *T. cruzi* within host cells (3). While its exact function is unknown, it is likely involved in the degradation of proteins scavenged from the blood meal of the insect vector (1).

The computer-assisted, rational search for new drugs has emerged as a popular strategy for the development of new chemotherapeutic agents. It involves both target- and ligand-based approaches. In particular, virtual screening (VS) has proven to be very useful in the discovery of new chemical entities for common as well as neglected diseases (4). A VS campaign led to the 2-hydrazolyl-4-thiazolidinone core as a potential cruzipain inhibitor. Based on this result, we designed, synthesized, and biologically evaluated a series of analogs against cruzipain and epimastigotes of *T. cruzi*. Computational tools were used to correlate the biological responses with physicochemical parameters of the compounds and to simulate the cruzipain–inhibitor interactions by docking calculations.

Methods and Materials

Chemistry

Reactions were monitored by analytical thin-layer chromatography (TLC) on 0.25-mm silica gel-coated plastic sheets (Polygram® SIL G/UV 254; Macherey-Nagel Düren, Germany). Flash chromatography on Silica gel 60 (J. T. Baker, 40 μm average particle diameter) was used to purify the crude reaction mixtures. ^{1}H and ^{13}C NMR spectra were recorded at 400 and 100 MHz, respectively, on a Bruker AVANCE. Chemical shifts (δ) are in ppm relative to the residual solvent signal, and coupling constants (J) are reported in Hz. Decoupled HMBC spectra were obtained using the Bruker hmbcgplpndqf pulse sequence using standard parameters. IR spectra were obtained on a Perkin Elmer 1310 (Wellesley, MA, USA) and Shimadzu 8101A FTIR spectrophotometers (Salem, OR, USA). Low-resolution mass spectra were measured on a GCMS Shimadzu QP 1100-EX spectrometer. High-resolution mass spectra were measured on VG AutoSpect spectrometer (EI mode). Microwave-assisted reac-

tions were carried out on a CEM Discover microwave reactor equipped with 10-mL vials. Melting points were determined using a Laboratory Devices Gallenkamp (Loughborough, Leicestershire, UK). All reactions were carried out in dry, freshly distilled solvents under anhydrous conditions unless otherwise stated. Yields are reported for chromatographic and spectroscopic (^{1}H and ^{13}C-NMR) pure compounds unless otherwise stated.

(1f–n) General procedure for the preparation of thiazolidineacetamides

The preparation of compound **1f** is representative.

(1f) (*RS*)-2-((2-(Benzylidene)hydrazono)-4-oxo-5-thiazolidine-*N*-methylacetamide

To a stirred solution of benzaldehyde (200 mg, 1.9 mmol) in PhMe (1 mL) and DMF (1 mL) were added thiosemicarbazide **3** (136 mg, 1.5 mmol) and *p*-TsOH acid (2 mg, 0.01 mmol). The reaction mixture was heated in stirred microwave vial for 3 min at 90 °C. After formation of thiosemicarbazone derivate, (followed by TLC) maleimide (138 mg, 1.26 mmol) was added, and the reaction mixture was heated 10 min at 110 °C in the microwave. The residue was finally recrystallized from MeOH/H_2O (1:1) to give **1f** (237 mg, 65% yield) as a white solid: mp 253–254 °C dec.; IR (KBr) 3321, 1712, 1644, 1569 cm^{-1}; ^{1}H NMR (DMSO-d_6) 2.60 (d, J = 4.6, 3H), 2.64 (dd, J = 16.2, J = 9.9, 1H), 2.94 (dd, J = 16.2, J = 3.7, 1H), 4.32 (dd, J = 9.9, J = 3.7, 1H), 7.47 (m, 3H), 7.76 (m, 2H), 8.00 (d, J = 4.6, 1H), 8.40 (s, 1H), 11.94 (bs, 1H); ^{13}C NMR (DMSO-d_6) 25.9, 37.8, 44.1, 127.4, 127.7, 128.7, 128.9, 130.7, 134.3, 156.1, 164.7, 169.3, 175.9; HRMS calculated for $C_{13}H_{14}N_4O_2S$ [M−H]$^+$: 291.0916, found: 291.0918.

(1g) (*RS*)-2-(2-(Thiophen-2-ylmethylene) hydrazono)-4-oxo-5-thiazolidine-*N*-methylacetamide

The typical procedure for thiazolidinone **1f** preparation was followed using 2-thiophenecarboxaldehyde to give thiazolidinone **1g** (75% yield) as a yellowish solid: mp 246–247 °C dec.; IR (KBr) 3324, 1712, 1640, 1571 cm^{-1}; ^{1}H NMR (DMSO-d_6) 2.59 (d, J = 4.7, 3H), 2.64 (m, 1H), 2.92 (dd, J = 16.1, J = 3.5, 1H), 4.29 (dd, J = 9.7, J = 3.5, 1H), 7.16 (m, 1H), 7.49 (d, J = 4.2 1H), 7.68 (dd, J = 4.2, J = 0.8, 1H), 7.97 (d, J = 4.7, 1H), 8.54 (s, H), 11.82 (bs, 1H); ^{13}C NMR (DMSO-d_6) 25.5, 37.8, 44.0, 128.0, 129.7, 132.7, 138.9, 150.5, 164.8, 169.7, 176.2; HRMS calculated for $C_{11}H_{12}N_4O_2S_2$ [M−H]$^+$: 297.0480, found: 291.0487.

(1h) (*RS*)-2-(2-(4-Methoxybenzylidene)hydrazono)-4-oxo-5-thiazolidine-*N*-methylacetamide

The typical procedure for thiazolidinone **1f** preparation was followed using *p*-OMe-benzaldehyde to give thiazolidinone **1h** (81% yield) as a white solid: mp 250–251 °C; IR (KBr) 3320, 1714, 1641, 1613, 1513 cm^{-1}; ^{1}H NMR (DMSO-d_6) 2.59 (d, J = 4.6, 3H), 2.64 (m, 1H), 2.92 (dd, J = 16.1, J = 3.7, 1H), 3.81 (s, 3H), 4.29 (dd, J = 9.9, J = 3.7, 1H), 7.01 (d, J = 8.8, 2H), 7.70 (d, J = 8.8, 2H), 7.99 (d, J = 4.6, 1H), 8.31 (d, J = 3.0, 1H), 11.86 (bs, 1H); ^{13}C NMR (DMSO-d_6) 25.6, 37.9, 44.0, 55.4, 78.7–79.3, 114.4, 126.9, 129.3, 155.7, 161.3, 169.2; HRMS calculated for $C_{14}H_{16}N_4O_3S$ [M−H]$^+$: 321.1021, found: 321.1022.

(1i) (*RS*)-2-(2-(4-Chlorobenzylidene)hydrazono)-3-methyl-4-oxo-5-thiazolidine-*N*-methylacetamide

The typical procedure for thiazolidinone **1f** preparation was followed using *p*-Cl benzaldehyde and methylthiosemicarbazide to give thiazolidinone **1i** (88% yield) as a white solid: mp 225–226 °C; IR (KBr) 3305, 1717, 1646, 1621, 1578 cm^{-1}; ^{1}H NMR ($CDCl_3$) 2.68 (dd, J = 16.1, J = 10.2, 1H), 2.87 (d, J = 4.8, 3H), 3.17 (dd, J = 16.1, J = 3.8, 1H), 3.33 (s, 3H), 4.38 (dd, J = 10.2, J = 3.8, 1H), 5.58 (s, 1H), 7.39 (d, J = 8.5, 2H), 7.71 (d, J = 8.5, 2H), 8.38 (s, 1H); ^{13}C NMR (DMSO-d_6) 26.4, 30.2, 38.5, 44.0, 129.9, 130.2, 133.9, 136.1, 157.0, 166.0, 170.0, 175.1; HRMS calculated for $C_{14}H_{15}ClN_4O_2S$ [M+Na]$^+$: 361.0496, found 361.0498.

(1j) (*RS*)-2-(2-(2-Bromobenzylidene)hydrazono)-3-methyl-4-oxo-5-thiazolidine-*N*-methylacetamide

The typical procedure for thiazolidinone **1f** preparation was followed using *o*-Br-benzaldehyde and methylthiosemicarbazide to give thiazolidinone **1j** (55% yield) as a white solid: mp 208–209 °C; IR (KBr) 3318, 1716, 1644, 1623, 1609 cm^{-1}; ^{1}H NMR (DMSO-d_6) 2.58 (d, J = 4.2, 3H), 2.71 (dd, J = 16.4, J = 9.6, 1H), 2.98 (dd, J = 16.4, J = 3.6, 1H), 3.19 (s, 3H), 4.39 (dd, J = 9.6, J = 3.6, 1H), 7.43 (m, 1H), 7.49 (t, J = 16.0, J = 8.0, 1H), 7.73 (d, J = 8.0, 1H), 7.98 (d, J = 8.0, 1H), 8.04 (d, J = 4.2, 1H), 8.67 (s, 1H); ^{13}C NMR (DMSO-d_6) 26.0, 29.9, 37.9, 43.6, 124.5, 128.4, 128.7, 132.9, 133.0, 133.8, 155.8, 166.9, 169.6, 174.7; HRMS calculated for $C_{14}H_{15}BrN_4O_2S$ [M+Na]$^+$: 404.9997, found: 404.9986.

(1k) (*RS*)-2-(2-(4-Fluorobenzylidene)hydrazono)-3-methyl-4-oxo-5-thiazolidin-*N*-methylacetamide

The typical procedure for thiazolidinone **1f** preparation was followed using *p*-F-benzaldehyde and methylthiosemicarbazide to give thiazolidinone **1k** (65% yield) as a white solid: mp 226–227 °C; IR (KBr) 2957, 1721, 1698, 1630 cm^{-1}; ^{1}H NMR (DMSO-d_6) 2.59 (d, J = 4.6, 3H), 2.70 (dd, J = 16.3, J = 9.7, 1H), 2.97 (dd, J = 16.3, J = 3.7, 1H), 3.17 (s, 3H), 4.37 (dd, J = 9.7, J = 3.7, 1H), 7.32 (t, J = 12.4, J = 5.4, 2H), 7.85 (m, 2H), 8.03 (d, J = 4.6, 1H), 8.51 (s, 1H); ^{13}C NMR (DMSO-d_6) 26.0, 29.8, 38.1, 43.6, 116.4 (d, J_{CF} = 22), 130.4 (d, J_{CF} = 9), 131.3 (d, J_{CF} = 3), 156.6, 164.5 (d, J_{CF} = 245), 165.2, 169.6, 174.6; HRMS calculated for $C_{14}H_{15}FN_4O_2S$ [M+H]$^+$: 323.0978, found: 323.0973.

(1l) (*RS*)-2-(2-(3-Bromobenzylidene)hydrazono)-3-methyl-4-oxo-5-thiazolidine-*N*-methylacetamide

The typical procedure for thiazolidinone **1f** preparation was followed using *m*-Br-benzaldehyde and methylthiosemicarbazide to give thiazolidinone **1l** (75% yield) as a white solid: mp 214–215 °C; IR (KBr) 3309, 1717, 1644, 1621, 1571 cm^{-1}; ^{1}H NMR ($CDCl_3$) 2.71 (dd, J = 16.0, J = 10.1, 1H), 2.88 (d, J = 4.8, 3H), 3.19 (dd, J = 16.0, J = 3.7, 1H), 3.35 (s, 3H), 4.39 (dd, J = 10.1, J = 3.7, 1H), 5.62 (s,

1H), 7.30 (m, 2H), 7.56 (ddd, J = 7.9, J = 1.8, J = 1.0, 1H), 7.68 (d, J = 7.9, 1H), 7.94 (d, J = 1.8, 1H), 8.36 (s, 1H); ^{13}C NMR ($CDCl_3$) 26.6, 29.8, 39.4, 43.5, 122.9, 126.9, 130.2, 130.6, 133.6, 136.3, 156.8, 165.0, 169.3, 174.3; HRMS calculated for $C_{14}H_{15}BrN_4O_2S$ $[M+H]^+$: 383.0177, found 383.0171.

(1m) (*RS*)-2-(2-(1-(3-Bromophenyl) ethylidene)hydrazono)-3-methyl-4-oxo-5-thiazolidine-5-*N*-methylacetamide

The typical procedure for thiazolidinone **1f** preparation was followed using *m*-Br phenylacetophenone and methylthiosemicarbazide to give thiazolidinone **1m** (88% yield) as a yellowish solid: mp 181–182 °C; IR (KBr) 3313, 1706, 1644, 1609, 1571 cm^{-1}; ^{1}H NMR (DMSO-d_6) 2.43 (s, 3H), 2.58 (d, J = 4.6, 3H), 2.71 (dd, J = 16.3, J = 9.5, 1H), 2.97 (dd, J = 16.3, J = 3.6, 1H), 3.21 (s, 3H), 4.36 (dd, J = 9.5, J = 3.6, 1H), 7.43 (t, J = 16.0, J = 8.0, 1H), 7.66 (d, J = 8.0, 1H), 7.86 (d, J = 8.0, 1H), 8.01 (t, J = 1.8, 1H); ^{13}C (DMSO-d_6) 14.4, 25.5, 29.4, 37.6, 43.1, 121.9, 125.5, 128.8, 130.7, 132.5, 140.0, 160.0, 164.2, 169.1, 174.2; HRMS calculated for $C_{15}H_{18}BrN_4O_2S$ EIMS $[M+H]^+$: 397.0334, found: 397.0338.

(1n) (*RS*)-2-(2-(4-Trifluoromethyl)benzy lidene)hydrazono)-3-methyl-4-oxo-5-thiazolidin-*N*-methylacetamide

The typical procedure for thiazolidinone **1f** preparation was followed using *p*-CF_3-benzaldehyde and methylthiosemicarbazide to give thiazolidinone **1n** (90% yield) as a white solid: mp 220–221 °C; IR (KBr) 3294, 1719, 1644, 1623, 1586, 1559 cm^{-1}; ^{1}H NMR ($CDCl_3$) 2.69 (dd, J = 23.1, J = 12.0, 1H), 2.87 (d, J = 4.5, 3H), 3.18 (dd, J = 23.1, J = 3.7, 1H), 3.34 (s, 3H), 4.38 (dd, J = 12.0, J = 3.7, 1H), 5.66 (d, J = 4.5, 1H), 7.66 (d, J = 8.2, 2H), 7.88 (d, J = 8.2, 2H), 8.45 (s, 1H); ^{13}C NMR ($CDCl_3$) 26.6, 29.8, 39.3, 43.5, 125.7 (q, J_{CF3} = 4 Hz), 126.5 (q, J_{CF3} = 262 Hz), 128.3, 131.9 (q, J_{CF3} = 32 Hz), 137.5, 156.7, 165.4, 169.3, 174.3; HRMS calculated for $C_{15}H_{15}F_3N_4O_2S$ $[M+H]^+$: 373.0946 373.0947.

(6a–e) General procedure for α, β-unsaturated thiazolidine esters

The preparation of compound **6c** is representative.

(6c) (*Z*)-2-(4-Fluorobenzylidene)hydrazono)-3-methyl-5-methoxycarbonylmethylene) thiazolidin-4-one

To a stirred solution of *p*-F-benzaldehyde (150 mg, 1.2 mmol) in dry EtOH (5 mL) were added methylthiosemicarbazide (140 mg, 1.3 mmol) and *p*-TsOH acid (15 mg, 0.1 mmol). After formation of methylthiosemicarbazone derivate (followed by TLC) was added dimethyl acetylenedicarboxylate (189 mg, 1.3 mmol). The reaction mixture was stirred at RT for 2 h, and a yellow precipitate was collected. The solid was recrystallized from ethyl acetate to give **6c** (304 mg, 81% yield) as yellow solid: mp 214–215 °C; IR (KBr) 3077, 1716, 1633, 1595 cm^{-1}; ^{1}H NMR ($CDCl_3$) 3.45 (s, 3H), 3.88 (s, 3H), 6.92 (s, 1H), 7.15–7.11 (m, 2H), 7.84–7.81 (m, 2H), 8.45 (s, 1H); ^{13}C NMR ($CDCl_3$) 29.7, 52.6, 115.9, 116.1, 130.1 (d, J_{CF} = 3), 130.4 (d, J_{CF} = 9), 141.8, 158.6, 160.6, 164.7 (d, J_{CF} = 252), 165.1, 166.5; HRMS calculated for $C_{14}H_{13}FN_3O_3S$ $[M+H]^+$: 322.0662, found: 322.0650.

(6a) (Z)-2-(4-Methoxybenzylidene)hydrazono-5-methoxycarbonylmethylene)thiazolidin-4-one

The typical procedure for thiazolidinone **6c** preparation was followed using *p*-OMe-benzaldehyde and thiosemicarbazide to give thiazolidinone **6a** (71% yield) as a yellow solid: mp 260–261 °C dec; IR (KBr) 2961, 1725, 1700 1643, 1606 cm^{-1}; ^{1}H NMR (DMSO-d_6) 3.79 (s, 3H), 3.82 (s, 3H), 6.67 (s, 1H), 7.06 (d, J = 8.8, 2H), 7.78 (d, J = 8.8, 2H), 8.46 (s, 1H); ^{13}C NMR (DMSO-d_6) 52.9, 55.9, 114.5, 114.9, 126.7, 130.3, 143.6, 158.8, 159.8, 162.2, 166.4.

(6b) (*Z*)-2-[4-Chlorobenzylidene)hydrazono]-3-methyl-5-methoxycarbonylmethylene) thiazolidin-4-one

The typical procedure for thiazolidinone **6c** preparation was followed using *p*-Cl-benzaldehyde to give thiazolidinone **6b** (85% yield) as a yellow solid: mp 204–205 °C; IR (KBr) 2949, 1711, 1703, 1621, 1581 cm^{-1}; ^{1}H NMR ($CDCl_3$) 3.45 (s, 3H), 3.88 (s, 3H), 6.92 (s, 1H), 7.41 (d, J = 8.5, 2H), 7.76 (d, J = 8.5, 2H), 8.43 (s, 1H); ^{13}C NMR ($CDCl_3$) 29.9, 52.7, 116.1, 129.2, 129.7, 132.4, 137.4, 141.8, 158.7, 161.0, 165.2, 166.6; HRMS calculated for $C_{14}H_{12}ClN_3O_3S$ $[M+Na]^+$: 360.0180, found: 360.0179.

(6d) (*Z*)-2-[(4-Trifluoromethyl) benzyliden)hydrazono]-3-methyl-5-methoxycarbonylmethylene) thiazolidin-4-one

The typical procedure for thiazolidinone **6c** preparation was followed using *p*-CF_3-benzaldehyde to give thiazolidinone **6d** (90% yield) as a yellow solid: mp 187–188 °C; IR (KBr) 2956, 1711, 1646, 1630 cm^{-1}; ^{1}H NMR ($CDCl_3$) 3.49 (s, 3H), 3.90 (s, 3H), 6.94 (s, 1H), 7.69 (d, J = 8.2, 2H), 7.94 (d, J = 8.2, 2H), 8.52 (s, 1H); ^{13}C NMR ($CDCl_3$) 29.8, 52.6, 116.3, 123.8 (q, J_{CF3} = 273), 125.7 (q, J_{CF3} = 4), 128.6, 132.6 (q, J_{CF3} = 33), 137.1, 141.5, 158.3, 161.9, 165.1, 166.5; HRMS calculated for $C_{15}H_{12}F_3N_3O_3S$ $[M+Na]^+$: 394.0444, found: 394.0443.

(6e) (Z)-2-(4-Methoxybenzylidene)hydrazono)-3-methyl-5-methoxycarbonylmethylene) thiazolidin-4-one

The typical procedure for thiazolidinone **6c** preparation was followed using *p*-OMe-benzaldehyde to give thiazolidinone **6e** (87% yield) as a yellow solid: mp 192–193 °C; IR (KBr) 2958, 1703, 1631, 1604 cm^{-1}; ^{1}H NMR ($CDCl_3$) 3.45 (s, 3H), 3.88 (d, J = 1.1, 6H), 6.91 (s, 1H), 6.96 (m, 2H), 7.78 (m, 2H), 8.43 (s, 1H); ^{13}C NMR ($CDCl_3$) 30.0, 52.8, 55.8, 114.6, 115.9, 126.9, 130.6, 142.4, 159.8, 162.6, 165.5, 166.9; HRMS calculated for $C_{15}H_{15}N_3O_4S$ $[M+H]^+$: 334.0856, found: 334.0856.

Cruzipain inhibitory activity

The activity was assayed in a reaction mixture (100 μL) containing in final concentration: Tris–HCl buffer, pH 7.6 (50 mM), Bz-Pro-Phe-Arg-pNA (0.150 mM), β-mercaptoethanol (10 mM) and cruzipain

(0.140 μM). Absorbance at 410 nm was monitored at 30 °C on a Beckman Model 25 spectrophotometer. The potential inhibitors were added as solutions in DMSO, and the control inhibitor was E64 (100% inhibition at 10 μM) added at same solvent concentration. All inhibitors were assayed by duplicate. The percentage of cruzipain inhibition (PCI) was calculated as follows: PCI (%) = $(A_i/A_0) \times 100$, where A_i and A_0 are the absorbance with and without inhibitor respectively.

Trypanocidal activity

Epimastigotes of the Tulhahuen 2 strain were grown at 28 °C in an axenic medium (BHT-Tryptose) complemented with 10% heat-inactivated fetal calf serum. Cells from 4-day-old culture (exponential phase) were inoculated to fresh medium to give an initial concentration of 13×10^6/mL. After the inoculation, each culture was supplemented with the inhibitors to a final concentration of 50 μM. Epimastigotes growth was monitored by counting the parasites in a Neubauer chamber.

The values given are means of parasite densities after 8 days. The final concentration of DMSO in the culture media was between 0.7% and 1.5%, the control was run in the same amount of DMSO and in the absence of any compound. The presence of up to 1.5% of DMSO in the culture medium does not have substantial effect on the epimastigote growth. The percentage of growth inhibition (PGI) was calculated as follows: inhibition (%) = $\{1-[(N_p-N_{0p})/(N_c-N_{0c})]\}\%$ 100, where N_p and N_{0p} is the number of cells of the culture containing the drug at 8 and 0 day respectively; N_c and N_{0c} is the number of cells of the culture in the absence of any drug at day 8 and at day 0 respectively.

Effects of inhibitors on the growth of Vero cells

Vero cells were seeded (10 000 cells/well) in 24-well cell culture cluster flat bottom (Corning) containing glass coverslips with 500 μL of MEM medium supplemented with 10% fetal calf serum. Cells were allowed to attach for 24 h in a humidified 5% CO_2/95% air atmosphere at 37 °C.

Then, the cells were exposed to the compounds (50 and 100 μM) for 24 h. Afterwards, the cell culture media was removed. Fresh MEM medium with 4% fetal calf serum and without inhibitors was added, and the coverslips were incubated at 37 °C for 48 h. The cells were then fixed and stained with May Grunwald–Giemsa. The effects of inhibitors in Vero cells at 100 μM inhibitor concentration were determined by contrast phase microscopy comparisons to Vero cells controls without inhibitor and classified as toxic and non-toxic.

Virtual screening

The methodology included a 2D QSAR approach based on application of linear discriminant analysis (LDA) and multiple linear regression (MLR) on 0D–2D molecular constitutional and topological descriptors from Dragon (Milano Chemometrics, 2003), including constitutional and topological descriptors, counts of functional groups, counts of fragments, information index, connectivity index, 2D autocorrelations and others. Detailed information on the models used is given in the Data S1.

Conformational analysis and docking

The conformational analysis of the tested compounds was carried out using the Conformational Search tool from the HyperChem 7.01 software package (Hypercube Inc, 2002). Geometry optimization was performed through molecular mechanics (MM + force field) with a gradient convergence threshold of 0.1 kcal/(Å mol). The five lowest-energy conformers were then refined at a semiempirical level with the PM3 base and a gradient convergence threshold of 0.05 kcal/(Å mol). The selected conformers were refined using Gaussian03 software (B3LYP/6-31G**). Charges were calculated at the same level of theory. The binding of compound **6b** to cruzain (Figure 3) was analyzed using AutoDockTools 1.5.2 and AutoDock 4.0 docking programs (5).

Results and Discussion

Synthesis

A VS strategy was applied to 537 503 chemical structures from the ZINC 5 database (6) to select new cruzipain inhibitors. 2-Hydrazolyl-4-thiazolidinone (**1**) cores were selected for synthesis, from the possible candidates. These are hybrid molecules that combine thiosemicarbazones with 4-thiazolidinones, two building blocks with interesting biological activities. The combination of both pharmacophores has been used to exhibit anti-*Toxoplasma gondii* (7), and also anti-*Trypanosoma cruzi* activity (8).

The selected scaffold **1** presents four regions to explore the chemical space: the substituents R^1 and R^2 at the hydrazolyl group, the substituent R^3 at the nitrogen of the thiazolidinone, the presence or absence of saturation at $\Delta^{5,6}$, and the substituent R^4 in the side chain (Figure 1).

We previously developed a Multicomponent Connection Reaction (MCR) for the synthesis of 2-hydrazolyl-4-thiazolidinones-5-carboxylic acids. Compounds **1a–e** were prepared using a tandem sequence assisted by microwave irradiation of a reaction mixture containing aldehydes (**2**, R^2 = H), thiosemicarbazide (**3**, R^3 = H) and maleic anhydride (**4**, X = O), see Table 1, entries 1–5 (9). The former process, compared to a stepwise reaction, allows the minimization of waste, amount of solvent, reagents, adsorbents, and energy.

A similar tandem sequence was applied for the synthesis of new 2-hydrazolyl-4-thiazolidinones amides **1f–n**, combining aldehydes or

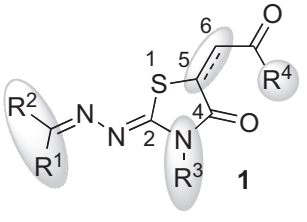

Figure 1: Hydrazolyl-4-thiazolidinones scaffold.

Table 1: Synthesis of thiazolidinones **1a–n**.

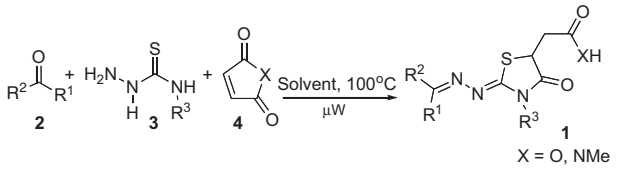

	Compounds	X	R^1	R^2	R^3	Yield (%)
1	**1a**	O	*p*-OMePh	H	H	61[a]
2	**1b**	O	2-thiophenyl	H	H	33[a]
3	**1c**	O	*o*-FPh	H	H	57[a]
4	**1d**	O	*p*-NO_2Ph	H	H	61[a]
5	**1e**	O	*p*-ClPh	H	H	70
6	**1f**	NMe	Ph	H	H	65[b]
7	**1g**	NMe	2-thiophenyl	H	H	75[b]
8	**1h**	NMe	*p*-OMePh	H	H	81[b]
9	**1i**	NMe	*p*-ClPh	H	Me	88[b]
10	**1j**	NMe	*o*-BrPh	H	Me	55[b]
11	**1k**	NMe	*p*-FPh	H	Me	65[b]
12	**1l**	NMe	*m*-BrPh	H	Me	75[b]
13	**1m**	NMe	*m*-BrPh	Me	Me	88[b]
14	**1n**	NMe	*p*-CF_3Ph	H	Me	90

[a]Reagents and conditions: PhMe/DMF, *p*-TsOH (cat.), 100 °C, μW.
[b]Reagents and conditions: PhMe, *p*-TsOH (cat.), 100 °C, μW.

ketones (**2**), hydrazides (**3**, R^3 = H or Me) and *N*-methylmaleimide (**4**, X = NMe), to give the desired amides in good yields (75–90% Table 1, see entries 6–14).

Finally, a series of new 2-hydrazolyl-4-thiazolidinone-5,6-α,β-unsaturated esters (**6**) was synthesized using an MCR between aldehydes **2**, thiosemicarbazides **3**, and dimethyl acetylenedicarboxylate **5**, to yield compounds **6a–e**, in EtOH at r.t. in excellent yields (71–90%), independent of the presence of electron-withdrawing or electron-donating groups, Table 2.

The reaction occurs first by thiosemicarbazone formation, followed by Michael addition of the sulfur atom to the triple bond and then cyclization to give in theory two possible products thiazolidines **6** or

Table 2: Synthesis of thiazolidinones **6a–e**

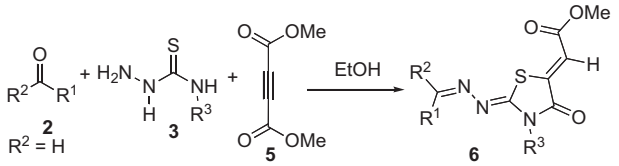

Compound	R^3	R^1	^3J(C,H) Hz	Yield (%)
6a	H	*p*-OMePh	5.2	71
6b	Me	*p*-ClPh	5.2	85
6c	Me	*p*-FPh	5.2	81
6d	Me	*p*-CF_3Ph	6.3	90
6e	Me	*p*-OMePh	5.2	87

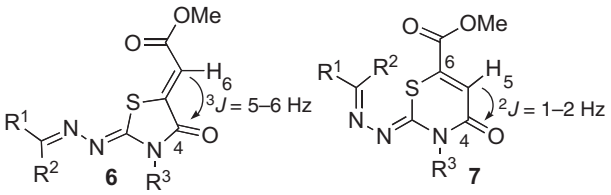

Figure 2: Thiazolidine **6** and 1,3-thiazine **7** isomers.

thiazines **7**, see Figure 2. The discrimination by ^{1}H-NMR and ^{13}C-NMR for compound **6** or **7** is not trivial, because they have almost identical signals in the spectra. A useful technique for the identification of the two possible isomers was the decoupled HMBC experiment to measure the coupling constant at 3 bonds (10). The ^3J values between H_6 and C_4 for all products **6a–e** were 6.3 to 5.2 Hz, and according to the literature these values correspond to an *exo* double bond in thiazolidines **6** (11) (see Table 2). Depending on the solvent used, a mixture of compounds **6** and **7,** in PhMe, or only the thiazolidinone **6** (in EtOH) was obtained.

All the compounds were prepared using a one-pot methodology and provided the desired structures in good yields from readily accessible starting materials.

Cruzipain inhibition

Different thiazolidinone derivatives including carboxylic acids **1a–e**, acetamides **1f–n** and α,β-unsaturated esters **6a–e** were evaluated against the cruzipain enzyme (12). Only thiazolidines **6b–e**, bearing an α,β-unsaturated ester, showed interaction with the enzyme at μM concentration (entries 16–18, Table 3); the remaining thiazolidinones were less active.

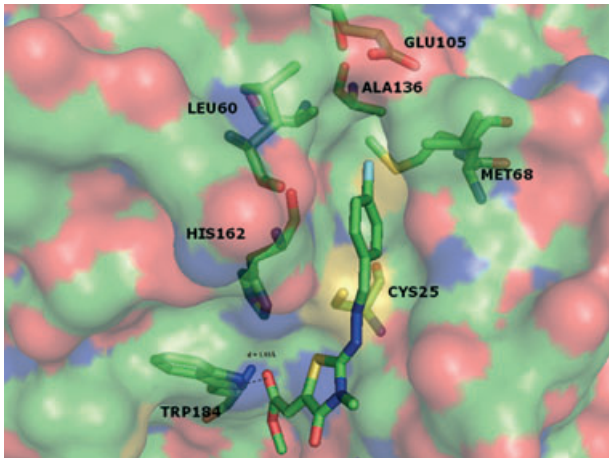

Figure 3: Surface representation of the active site of cruzain. Ligand and important residues were highlighted as stick representations. Hydrogen atoms are not shown. Colored atoms are as follows: Carbon atoms in green, nitrogen atom in blue, oxygen atoms in red, sulfur atoms in yellow, and chlorine atoms in light blue. Hydrogen bond interaction d = 1.93Å.

Table 3: Biological activities of synthetic thiazolidinones **1a–n**, and **6a–e** against cruzipain.

Entry	Compound	PCI (%)[a]	Entry	Compound	PCI (%)[a]	Entry	Compound	PCI (%)[a]
1	**1a**	36	8	**1h**	22	15	**6a**	7
2	**1b**	34	9	**1i**	7	16	**6b**	75
3	**1c**	6	10	**1j**	0	17	**6d**	65
4	**1d**	4	11	**1k**	3	18	**6e**	71
5	**1e**	11	12	**1l**	17	19	**6c**	0
6	**1f**	3	13	**1m**	22	20	**E-64**	100
7	**1g**	27	14	**1n**	27	–	–	–

[a]PCI = % of cruzipain inhibition at (Inhibitor) = 100 μM, (Cruzipain) = 0.140 μM, values are means of two values.
E64: trans-Epoxysucciny-L-leucyl-amido(4-guanidino) butane; (L-3-*trans*-Carboxyoxiran-2-Carbonyl)-L-Leucyl-Admat was used as reference compound.

Anti-Trypanosoma cruzi activity and toxicity

According to these assays, a subset of selected compounds was evaluated in their capability to inhibit the epimastigote form of *T. cruzi* (Tulahuen 2, strain) growth, (Table 4). A good correlation between in vitro anti-*T. cruzi* epimastigote and in vivo anti-*T. cruzi* activities has been reported (13); therefore, we used this biological test to validate our possible hits.

It is interesting to note that related thiazolidinones were predicted by Lima *et al.* (8) as potential cruzipain inhibitors based on docking calculations, and their activity was supported by anti-*T. cruzi* (epimastigotes) assays. Our results pointed toward a different scenario; the antiparasitic activity of this core is independent of the cruzipain inhibition. The most active compounds against *T-cruzi* Tul-2 **1i, j, k, m** are inactive at the enzyme, so this activity is indeed independent on the cystein protease activity. Thiazolidinone **6c** is the only compound active in both assays. We can conclude that these compounds involve a different mechanism of action. The best results for anti-*T. cruzi* activity were obtained with the compounds **1** or **6**, having as substituents: R^3 = Me; R^2 = H or Me; R^1 = Ph bearing an halogen, independent of the presence or absence of the $\Delta^{5,6}$ alkene.

Furthermore, compounds **1a–n** and **6a–e** were also evaluated using epimastigotes Y, a resistant strain against Nifurtimox and Benznidazole, but only compound **6d** showed a moderate activity (PGI-Y = 37% at 50 μM) (14).

Table 4: Anti-*Trypanosoma cruzi* Tulahuen 2 and cytotoxic activities

Compound	Inhibition[a] (%) Tul2	Cytotoxic category[b]	Compound	Inhibition[a] (%) Tul2	Cytotoxic category[b]
1a	0	nd	**1m**	60	Non-toxic
1b	0	nd	**1n**	42	Non-toxic
1c	0	nd	**6b**	39	Toxic
1d	0	nd	**6c**	50	Toxic
1i	50	Toxic	**6d**	46	Toxic
1j	52	Toxic	**6e**	38	Non-toxic
1k	50	Toxic	**Nfx**[c]	100	nd
1l	28	Non-toxic	–	–	–

[a]Inhibition % was tested at 50 μM.
[b]Determined at 100 μM inhibitor concentration by contrast phase microscopy comparisons to Vero controls; nd = not determined.
[c]Nfx: Nifurtimox was used as reference drug.

The unspecific cytotoxicity for the most active compounds **1i–n** and **6b–e** was evaluated in vitro against mammalian cells at 100 and 50 μM, using Vero cells as the cellular model. The results showed that compounds **1l, 1m,** and **1n** were non-toxic at the highest doses assayed, and compound **1m** was found to have the best selectivity as anti-*T. cruzi* Tul 2 agent, see Table 4.

Molecular modeling and QSAR studies

The mechanistic proposal for cruzipain inhibition involves a nucleophilic attack of the cysteine sulfur atom to an electrophilic moiety able to accept electrons. According to this idea, we decided to gain insight into the atomic distribution of charges as well as the contribution of each atom to the frontier orbital. A systematic conformational analysis and ab *initio* geometry optimization was carried out as described in the experimental section. The electronic parameters computed were HOMO and LUMO energies, LUMO and HOMO coefficients, normalized LUMO and HOMO coefficients for each atom (15). Common physicochemical properties are frequently related to biological activity and the drug-likeness concept, such as theoretical logP (Moriguchi's LogP–mlogP), $(mlogP)^2$, molecular refractivity (MR) and molecular weight (MW), which also calculated using DRAGON software.

The QSAR analysis showed a very poor correlation between cruzipain inhibition (PCI) and the calculated descriptors.

However, better results were obtained between PGI-Tul2 activity and the descriptors, revealing significant correlations with MR (correlation coefficient $r = 0.83$), Moriguchi's logP ($r = 0.79$), and $(mlogP)^2$ ($r = 0.74$). The MR explained around 70% of the variance of the 14 assayed compounds.

Docking

Molecular docking was used to analyze the binding mode of **6b**, the most active compound of the set. The most stable docking conformation obtained for **6b** is shown in Figure 3. A hydrogen-bonding interaction was predicted between the ester group of the inhibitor and the TRP184 residue, with a 1.93 Å measured distance. Additionally, the aromatic ring of **6b** makes positive lipophilic interactions with the hydrophobic S2 pocket of the enzyme, characterized by LEU60, ALA136, and MET68 residues. The chlorine atom points toward the end of the cavity, delimited by the GLU105 residue, which is capable of extending its carboxylic group out to avoid negative interactions with lipophilic ligands. Despite these nonbonded interactions that stabilized the complex, no interactions were found between **6b** and the CYS25 and/or HIS162 catalytic residues and no nucleophilic attack can be predicted. This observation may explain the observed weak inhibition of cruzipain.

Conclusions

New 2-hydrazoyl-4-thiazolidinone scaffolds could be obtained from commercially available starting materials by using MCR and well-

established methodologies. Compounds **1i, 1j, 1k, 1m,** and **6c** showed the highest antiproliferative activity when screened on *T. cruzi*-Tul2. Compound **6b** was the most active on cruzipain but only moderately active on the parasite. The mode of action proposed for these compounds is based on a different mechanism rather than cruzipain inhibition. Toxicity screening was also performed pinpointing the amide **1m** as the most selective compound. Further structure optimization is needed to increase the antichagasic activity.

Docking calculation of the compounds allowed explaining, on a molecular basis, why the selected inhibitors were only able to inhibit cruzipain at the μM level. Inhibitor **6b** seems to interact with the hydrophobic pocket of the enzyme, and no nucleophilic attack was predicted.

QSAR analysis showed significant correlations between mlogP and MR versus anti-*T. cruzi* Tul 2 activity. One might infer that these correlations could be associated with permeation through the parasite cellular membrane. Remarkably, the best-correlated descriptors are usually used to characterize permeability and bioavailability.

These results might be used in an iterative way to construct new, refined models with improved predictive capability, to conduct new virtual screening campaigns.

Acknowledgments

This work was supported by the National Institutes of Health-FIRCA (R03TW007772). We greatly appreciate Prof. Mercedes González for providing valuable suggestions and corrections to this paper. G.M. thanks RIDIMEDCHAG-CYTED. A.T., L.G., and J.J.C. are members of the Research Career of CONICET (Argentina). L.B.-B. and L.G. thank ANPCyT and Incentivos UNLP. P.P. thanks CIC-BsAs.

References

1. McKerrow J.H., Doyle P.S., Engel J.C., Podust L.M., Robertson S.A., Ferreira R., Saxton T., Arkin M., Kerr I.D., Brinen L.S., Crack C.S. (2009) Two approaches to discovering and developing new drugs for Chagas disease. Mem Inst Oswaldo Cruz;104:263–269.
2. Cazzulo J., Stoka V., Turk V. (2001) The major cysteine proteinase of *Trypanosoma cruzi*: a valid target for chemotherapy of Chagas disease. Curr Pharm Design;7:1143–1156.
3. Franke de Cazzulo B.M., Martinez J., North M.J., Coombs G.H., Cazzulo J.J. (1994) Effect of proteinase inhibitors on the growth and differentiation of *Trypanosoma cruzi*. FEMS Microbiol Lett;124:81–86.
4. Ferreira R., Simeonov A., Jadhav A., Eidam O., Mott B.T., Keiser M.J., McKerrow J.H., Maloney D.J., Irwin J., Shoichet B.K. (2010) Complementarity between a docking and a high-throughput screen in discovering new Cruzain inhibitors. J Med Chem;53:4891–4905.
5. Morris G.M., Goodsell D.S., Halliday R.S., Huey R., Hart W.E., Belew R.K., Olson A.J. (1998) Automated docking using a Lamarckian genetic algorithm and empirical binding free energy function. J Comput Chem;19:1639–1662.
6. Irwin J.J., Shoichet B.K. (2005) ZINC – a free database of commercially available compounds for virtual screening. J Chem Inf Model;45:177–182.
7. de Aquino T.M., Liesen A.P., da Silva R.E.A., Lima V.T., Carvalho C.S., de Faria A.R., de Araujo J.M., de Lima J.G., Alves A.J., de Melo E.J.T., Goes A.J.S. (2008) Synthesis, anti-*Toxoplasma gondii* and antimicrobial activities of benzaldehyde 4-phenyl-3-thiosemicarbazones and 2-[(phenylmethylene)hydrazono]-4-oxo-3-phenyl-5-thiazolidineacetic acids. Bioorg Med Chem;16:446–456.
8. Lima A.C., Souza R., Moreira D.R., Cardoso M.V.O., Gouveia A.C., Farias L.M., Zaldini M., Costa A., Santana R., Soares M.B.P. (2006) Synthesis, docking, and in vitro activity of thiosemicarbazones, aminoacyl-thiosemicarbazidesand acyl-thiazolidones against *Trypanosoma cruzi*. Bioorg Med Chem;14:3749–3757.
9. Saiz C., Pizzo C., Manta E., Wipf P., Mahler S.G. (2009) Microwave assisted tandem reactions for the synthesis of 2-hydrazolyl-4-thiazolidinones. Tetrahedron Lett;50:901–904.
10. Laughlin M.R., Taylor J., Chesnick A.S., Balaban R.S., Summers M.F., Marzilli L.G., Bax A. (1986) Complete H-1 and C-13 assignments of coenzyme-B12 through the use of new two-dimensional NMR experiments. J Am Chem Soc;108:4285–4294.
11. Vogeli U., Philipsborn W. (1978) Structures of addition products of acetylenedicarboxylic acid esters with various dinucleophiles. An application of C,H-spin-coupling constants. Helv Chim Acta;61:607–617.
12. Labriola C., Sousa M., Cazzulo J.J. (1993) Purification of the major cysteine proteinase (cruzipain) from *Trypanosoma cruzi* by affinity chromatography. Biol Res;26:101–112.
13. Boiani L., Gerpe A., Arán V.J., Torres de Ortiz S., Serna E., Vera de Bilbao N., Sanabria L., Yaluff G., Nakayama H., Rojas de Arias A., Maya J.D., Morello A., Cerecetto H., González M. (2009) In vivo studies of 5-arylethenylbenzofuroxans in acute murine models of Chagas disease. Eur J Med Chem;44:1034–1040.
14. Porcal W., Hernández P., Aguirre G., Boiani L., Boiani M., Merlino A., Ferreira A., Di Maio R., Castro A., González M., Cerecetto H. (2007) Second generation of 5-ethenylbenzofuroxan derivatives as inhibitors of *Trypanosoma cruzi* growth: synthesis, biological evaluation, and structure–activity relationships. Bioorg Med Chem;15:2768–2781.
15. Locke J., Griffith R., Bailey T., Crumbie R. (2009) Competition between cyclization and bisimine formation in the reaction of 1,3-diaminopropanes with aromatic aldehydes. Tetrahedron;65:10685–10692.

Supporting Information

Additional supporting information may be found in the online version of this article.

Data S1. General procedure for the preparation and characterization of all new compounds.

Please note: Wiley-Blackwell is not responsible for the content or functionality of any supporting materials supplied by the authors. Any queries (other than missing material) should be directed to the corresponding author for the article.